Chemical Engineering Journal 175 (2011) 222–227

Contents lists available at SciVerse ScienceDirect

Chemical Engineering Journal

journal homepage: www.elsevier.com/locate/cej

Preparation and application of stability enhanced magnetic nanoparticles for rapid removal of Cr(VI)

Ya Pang[a,b], Guangming Zeng[a,b,*], Lin Tang[a,b,*], Yi Zhang[a,b], Yuanyuan Liu[a,b], Xiaoxia Lei[a,b], Zhen Li[a,b], Jiachao Zhang[a,b], Zhifeng Liu[a,b], Yiqun Xiong[a,b]

[a] College of Environmental Science and Engineering, Hunan University, Changsha, 410082 China
[b] Key Laboratory of Environmental Biology and Pollution Control (Hunan University), Ministry of Education, Changsha, 410082, China

ARTICLE INFO

Article history:
Received 6 July 2011
Received in revised form
21 September 2011
Accepted 21 September 2011

Keywords:
Magnetic nanoparticle
γ-Fe_2O_3
Chromium
Adsorption
Selectivity

ABSTRACT

A stable magnetic nanoparticle with a shell core structure of γ-Fe_2O_3@Fe_3O_4 was developed. Water soluble Polyethylenimine (PEI) was grafted to the nanoparticle to prepare a positive charged adsorbent, which was characterized by XRD, FTIR and SEM. The adsorbent was able to effectively remove anionic Cr(VI) in the pH range of 2–3 due to the large amount of protonated imine groups on its surface, and could be magnetically separated from liquid quickly. Adsorption equilibrium was reached within 30 min and independent of initial Cr(VI) concentration. The Cr(VI) maximum sorption capacity at a temperature range of 35–15 °C was obtained using the Langmuir adsorption isotherm. The calculated thermodynamic parameters (ΔG, ΔH, and ΔS) indicated that adsorption of Cr(VI) was spontaneous and exothermic in nature. Competition from coexisting ions (K^+, Na^+, Ca^{2+}, Cu^{2+}, Cl^-, and NO_3^-) was found insignificant. The adsorbent had satisfying acid–alkali stability and could be regenerated by 0.02 mol L^{-1} NaOH solution. The results suggested the potential application of the PEI-modified magnetic nanoparticles in selective removal of Cr(VI) from wastewater.

1. Introduction

Hexavalent chromium Cr(VI) is a highly toxic heavy metal, which is able to cause carcinogenesis, mutation to humans and animals, thus has been designated as one of the top-priority toxic pollutants by the U.S. EPA [1]. Metal finishing, electroplating, leather tanning, and chromate production are the main sources of Cr(VI) wastewater [2,3]. In some industry processes, the improper even untreated effluent was discharged randomly, leading to the Cr(VI) pollution. Therefore, developing effective method to removal Cr(VI) from effluent is of great importance to the public health and ecological system. Among the methods for Cr(VI) pollution remediation, such as adsorption, electrochemical precipitation, ion exchange, and membrane filtration, adsorption is one of the most popular and effective options. Various natural materials such as bark, clay, seaweed and biomass, as well as synthetic adsorbent like activated carbon, resin, and mesoporous silica [4,5], have been used to remove heavy metals. Furthermore, regeneration of exhausted adsorbent with economy operation is possible, and in many cases, the treated effluent is suitable for reuse [5].

Recently, using nanosized magnetic material as adsorbent has attracted increasing interest due to their high surface area and unique superparamagnetism. For instance, Fe_3O_4 nanoparticle coated with humic acid was found to be an effective adsorbent for Hg, Pb, Cd, and Cu from wastewater [6]. Chitosan-bound Fe_3O_4 particles with a mean diameter of 13.5 nm were able to rapidly remove Cu [7]. Superparamagnetic Fe_3O_4 nanoparticles with a surface functionalization of dimercaptosuccinic acid were performed to bind Hg, Ag, Pb, Cd, and Ti availably [8]. For the above reported adsorbent, Fe_3O_4 nanoparticle is the magnetic source, however, it is susceptible to air oxidation, resulting in the loss of magnetization. Although coating the Fe_3O_4 with inorganic shell, such as silica [9] and carbon [10], was capable to improve its chemical stability, the magnetic response of adsorbent would decrease after coating. An effective way to solve the contradiction between chemical stability and magnetic response is to calcine Fe_3O_4 nanoparticles to obtain a good crystalline [11].

In this study, prepared Fe_3O_4 was submitted to calcinations to form γ-Fe_2O_3@Fe_3O_4 magnetic nanoparticles. Polyethylenimine (PEI), which not only chelates cationic metal ions such as Cu^{2+}, Zn^{2+}, and Pb^{2+} [4,12], but also binds metal oxyanion through electrostatic interaction [2], was chosen to modify the particles. The adsorbent was positive charged over a wide pH range, and Cr(VI) exists in wastewater as negative charged anion, bringing about strong electrostatic interaction between adsorbent and adsorbate. The prepared PEI-modified magnetic adsorbent was characterized

* Corresponding authors at: College of Environmental Science and Engineering, Hunan University, Changsha 410082, China. Tel.: +86 731 88822754; fax: +86 731 88823701.
E-mail addresses: zgming@hnu.cn (G. Zeng), tanglin@hnu.cn (L. Tang).

1385-8947/$ – see front matter © 2011 Elsevier B.V. All rights reserved.
doi:10.1016/j.cej.2011.09.098

by SEM, XRD, and FTIR. The sorption performances, such as kinetics, isotherms, thermodynamics, and competitive uptake were evaluated.

2. Materials and methods

2.1. Preparation of adsorbent

The Fe_3O_4 was prepared by the conventional chemical coprecipitation method [9]. Briefly, 0.4 mol of $FeCl_3{\cdot}6H_2O$ and 0.2 mol of $FeCl_2{\cdot}4H_2O$ were dissolved in 250 mL ultrapure water, soon the solution was bubbled with N_2 gas for 20 min to remove dissolved O_2. Then, 50 mL of 4 mol L^{-1} ammonia solutions were added under vigorous mechanical stirring to adjust the pH to about 10. The reaction was maintained at 65 °C for 30 min. The resulting black nanoparticles were separated by an external magnetic field followed by repeated washing with ultrapure water to neutrality. Finally, they were vacuum-desiccated at 55 °C. The dry nanoparticles were calcined at 300 °C for 1 h to gain red–brown magnetic nanoparticles (MNPs). Next, the MNPs were activated at 80 °C using 1.5 mol L^{-1} lauric acid solutions with pH 10. After washing with ethanol and water, the particles were added into 5% PEI in 50% methanol to covalently bind with PEI at 80 °C for 1 h. The developed adsorbent (abbreviated as PEI-MNPs) was thoroughly rinsed and then dried and ground for subsequent use.

2.2. Characterization of magnetic nanoparticles

The XRD patterns were performed on a Rigaku D/max-II B X-ray diffractometer with Cu Kα radiation (λ = 0.1541 nm) in the 2θ range of 10–80°. FTIR spectra were collected on a WQF-410 FTIR spectrometer, by accumulating 32 scans at a spectra resolution of 4 cm^{-1}, with the ration of sample to KBr of 1:100. Scanning electron microscope (SEM) images were obtained on a JEOL JSM-6700 equipped with energy dispersive spectroscopy (EDS). To prepare the samples, the nanoparticles were first added into water and sonicated for 15 min for dispersion. Then, 10 μL suspensions were dropped on conductive adhesive and dried. To measure the zeta potentials of the naked and PEI-bound MNPs, sample of 0.01 g was dispersed in 100 mL of 1 mmol/L NaCl solution to sonicate for 15 min. After placing for 24 h, the supernatant was used for zeta potential measurement using Malvern ZEN3600 Zetasizer Nano.

2.3. Batch adsorption experiments

Batch experiments were conducted in glass conical flasks by shaking at 150 rpm in a water bath shaker. Each treatment contained 0.08 g adsorbents and 20 mL of chromium solutions prepared with $K_2Cr_2O_7$. After finishing adsorption, the adsorbent was magnetically separated and the supernatant was collected for Cr(VI) measurement. The concentration of Cr(VI) was determined using UV–vis spectrophotometer (UV-754N shanghai, China) at 540 nm. All experiments were performed in duplicate with the averaged values reported here.

2.4. Stability and regeneration studies

Stability of the PEI-MNPs was examined by dispersing 0.08 g adsorbent in 20 mL different concentration of HCl or NaOH solution. After shaking for 3 h at 25 °C, the leached iron concentration was determined by AAS (Hitachi Z-8100, Japan). The treated adsorbent was washed to neutrality for reuse to infer its stability.

Desorption studies were conducted by incubation of 0.08 g Cr-loaded adsorbent in 15 mL of 0.02 mol L^{-1} NaOH solution for 1 h. To evaluate the regeneration, the eluted adsorbent was exploited to remove Cr(VI) again. Prior to the next adsorption–desorption cycle, the magnetic adsorbent was washed thoroughly with ultrapure water to neutrality and reconditioned for adsorption.

3. Results and discussion

3.1. Characterization of adsorbent

Fig. 1 shows the XRD pattern of the Fe_3O_4 nanoparticles. Six typical peaks for Fe_3O_4 ($2\theta = 30.1°$, 35.5°, 43.1°, 53.4°, 57.0°, and 62.6°), marked by their indices ((2 2 0), (3 1 1), (4 0 0), (4 2 2), (5 1 1), and (4 4 0)), were observed, which accorded well with the database (JCPDS 01-1111), demonstrating the successful synthesis of Fe_3O_4 nanoparticles with a cubic structure [11]. It was reported that γ-Fe_2O_3 can be produced by heating Fe_3O_4 to 300 °C [13]. The calcined Fe_3O_4 nanoparticles presented a red–brown, which was the characteristic color of the formed γ-Fe_2O_3 [14]. However, the XRD pattern for the calcined magnetic nanoparticle was very similar to that of the Fe_3O_4 (data not shown), implying that only superficial Fe_3O_4 transformed to γ-Fe_2O_3 as confirmed by previous studies [11,14–16]. Thus a shell core structure of γ-Fe_2O_3@ Fe_3O_4 was formed and applied to crosslink with PEI. FTIR spectroscopic analysis further proved the structure (Fig. 2a–c). The peaks at 580 cm^{-1} (Fig. 2a), belonging to Fe^{2+}–O^{2-} stretching vibration, changed to 563 cm^{-1} after the nanoparticle was calcined (Fig. 2b), implying that the Fe^{2+} was oxidized to Fe^{3+} [15]. In concomitance with the modification of PEI onto magnetic nanoparticles, new peaks at 1003, 1471, and 2941 cm^{-1} (Fig. 2c), representing the C–N stretching, C–H bending, and CH– stretching vibration, respectively, were

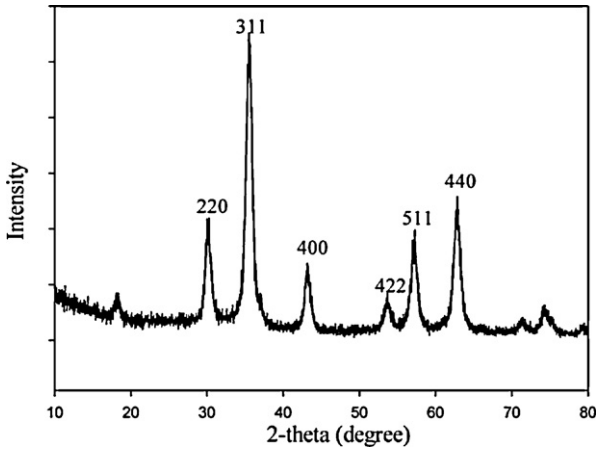

Fig. 1. XRD pattern of prepared Fe_3O_4 nanoparticles.

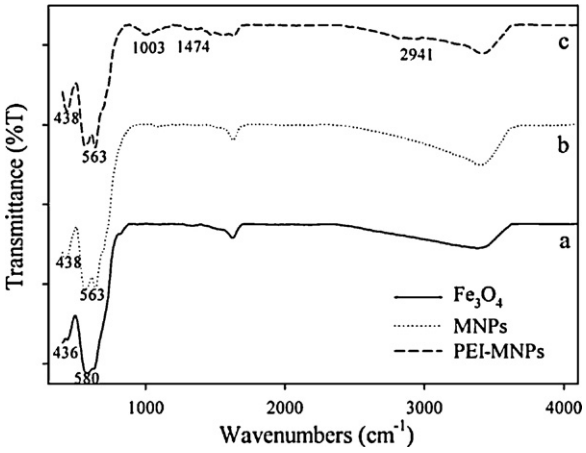

b]

Fig. 2. FTIR spectra: (a) Fe_3O_4 nanoparticles; (b) MNPs; (c) PEI-MNPs.

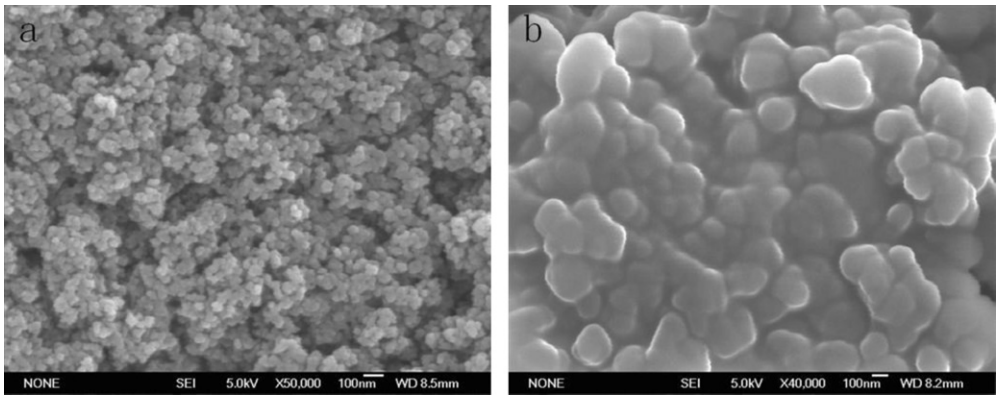

Fig. 3. SEM micrographs of (a) MNPs and (b) PEI-MNPs.

observed. These changes must be due to the imine groups in PEI [12], suggesting the introduction of PEI on the magnetic nanoparticles.

Fig. 3 presents the photomicrographs of MNPs before and after surface modification. The diameter of the particles after modification (Fig. 3b approximate 100 nm) was larger than that of the pristine magnetic ones (Fig. 3a approximate 40 nm), which was attributed to the graft of PEI. EDS analysis revealed that the content of N in adsorbent was 5.35% (w/w).

3.2. Effect of solution pH

The solution pH significantly influences the surface charge and the protonation degree of adsorbent. The zeta potential of the pristine and PEI-MNPs at different pH are shown in Fig. 4. The zero point of zeta potential (pH_{zpc}) for pristine particle had been found at pH 5.5. In contrast, the pH_{zpc} for the PEI-MNPs was increased to a much higher value of 11.4, which was attributed to the protonation of imine groups on the particle surface. In agreement with earlier study [2], the pH_{zpc} was significantly increased after the modification of PEI to the matrix surface.

In addition, Cr(VI) exists in solution as different ionic forms. The main Cr(VI) species are CrO_4^{2-}, $Cr_2O_7^{2-}$, and $HCrO_4^-$, depending on the solution pH and total chromate concentration [17,18]. Based on thermodynamic database [18], a predominance diagram for Cr(VI) using pH and total Cr(VI) concentration as variables is presented in Fig. 5. The two vertical lines divide the diagram into three parts, and the area between the two horizontal dashed stands for the Cr(VI) concentration ranging from 50 mg L^{-1} to 500 mg L^{-1}. As shown in it, $HCrO_4^-$ and CrO_4^{2-} are the predominant species

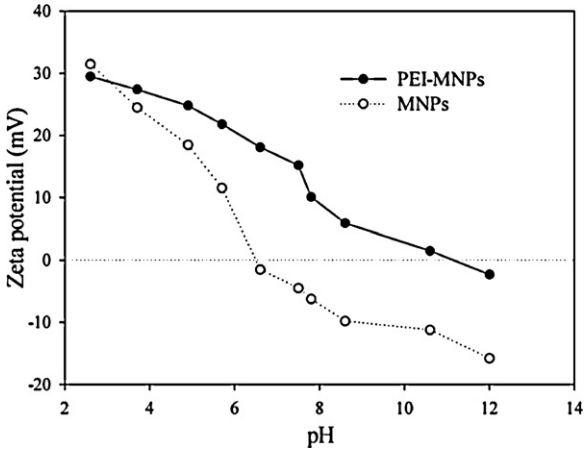

Fig. 4. Zeta potential of MNPs and PEI-MNPs as a function of pH.

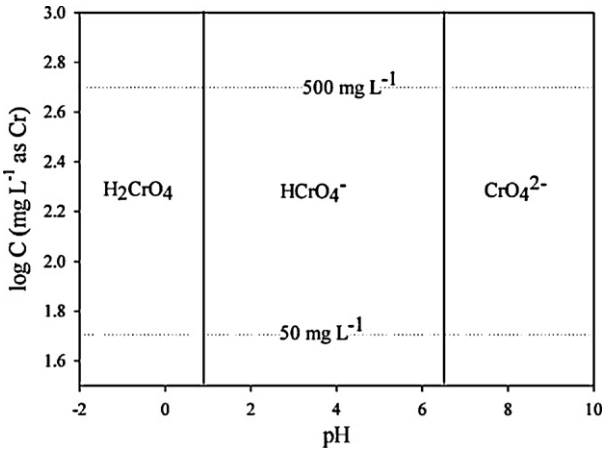

Fig. 5. Cr(VI) species in solution as a function of pH and total Cr(VI) concentration.

at the experimental total Cr(VI) concentration. For pH lower than 6.8, $HCrO_4^-$ is the dominant component of hexavalent chromium, and above pH 6.8, only CrO_4^{2-} existed.

The effect of pH on adsorption of Cr(VI) is shown in Fig. 6. The removal efficiency was more than 95% in the pH range of 2–3, subsequently, it decreased sharply in the solution pH range of 4–7, ultimately, less than 55% Cr(VI) was removed in the alkali solution. Therefore, pH value between 2 and 3 was an ideal parameter in this work. As the adsorbent was positively charged when the solution pH < 11.4, from the viewpoint of electrostatic

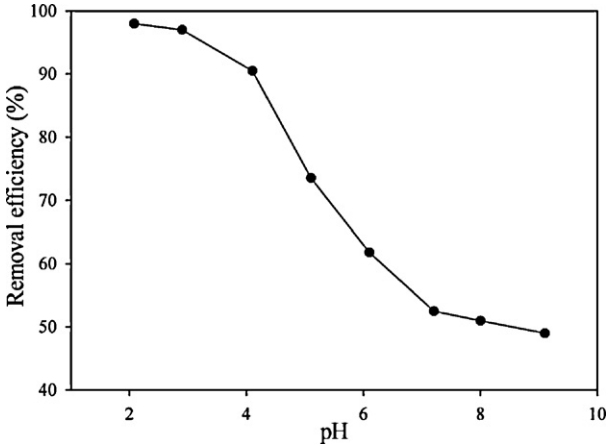

Fig. 6. Effect of pH on removal of Cr(VI) (metal concentration 100 mg L^{-1}, adsorbent dose 0.08 g, contact time 30 min, temperature 25 °C).

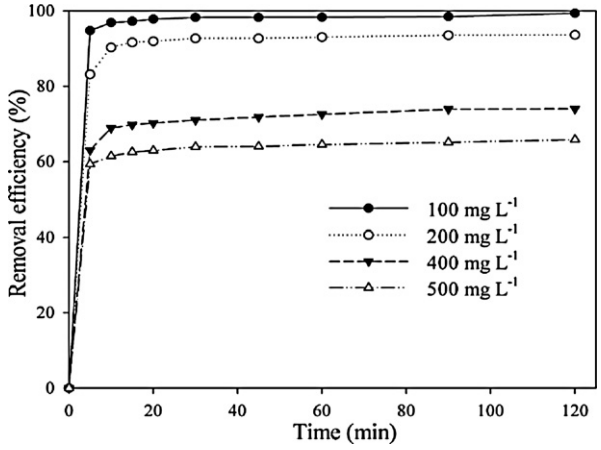

Fig. 7. Effect of contact time on removal of different initial concentrations Cr(VI) (adsorbent dose 0.08 g, pH value 2.2, temperature 25 °C).

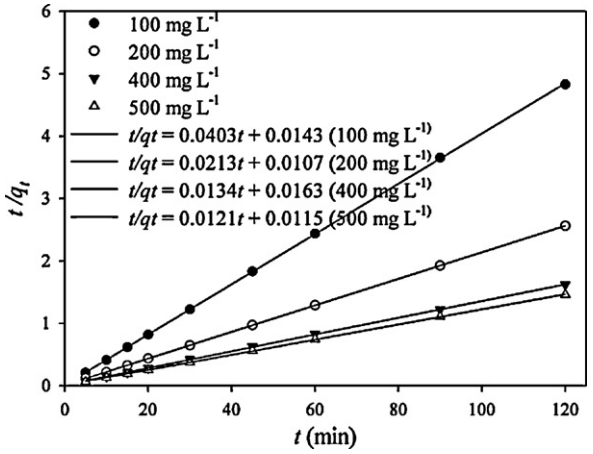

Fig. 8. Linear fit of experimental data using pseudo-second-order kinetic model.

interaction, lower pH was favourable to the adsorption of anionic Cr(VI). With the increase of pH, the zeta potential of the adsorbent decreased and the competition from –OH increased, resulting in the weak interaction between Cr(VI) and adsorbent, thus the removal efficiency decreased. Fig. 5 illustrated that the predominant form of Cr(VI) changed to CrO_4^{2-} from $HCrO_4^-$ at pH > 7. The adsorption free energy of CrO_4^{2-} (−2.1 to −0.3 kcal mol^{-1}) is higher than that of $HCrO_4^-$ (−2.5 to −0.6 kcal mol^{-1}) [19]. Consequently, CrO_4^{2-} is less likely adsorbed than $HCrO_4^-$ at the same concentration.

3.3. Effect of contact time on adsorption

The effect of contact time on removal of 100, 200, 400 and 500 mg L^{-1} Cr(VI) is shown in Fig. 7. The adsorption rate was considerably fast, with over 92% of the Cr(VI) removed in the first 10 min. The required equilibrium time for different initial concentrations had no significant difference, indicating a strong interaction between the adsorbent and adsorbate. The rapid adsorption performance of PEI-MNPs might be related to the properties of itself. Since the adsorbent was nanosized, a high surface area was provided for easy contacting between Cr(VI) and active site. In addition, the adsorbent was dispersed in solution evenly due to the water soluble nature of PEI, producing little external diffusion resistance [7,8], ultimately, bringing about fast adsorption equilibrium. However, the equilibrium time for Cr(VI) adsorption by some other adsorbents was much longer. For example, uptake of Cr(VI) by PEI-modified fungal biomass took 3–6 h to reach saturation [2], while 10–50 h was needed for activated carbon [20]. The maximum removal efficiency of Cr(VI) with initial concentration of 100, 200, 400, 500 mg L^{-1} reached 98.2%, 92.6%, 72.5%, and 64.6%, respectively, suggesting that the Cr(VI) removal efficiency decreased with the increase of initial concentration. This phenomenon was predictable due to the fact that the dosage of adsorbent was fixed, thus the total available active sites were limited, leading to the decrease of removal efficiency corresponding to an increased initial Cr(VI) concentration.

Adsorption kinetic model not only allows estimation of adsorption rate but also provides insights into rate expression characteristic of possible reaction mechanisms. It was pointed out that pseudo-second-order adsorption model was based on the assumption that the rate-controlling step, involving valence forces through sharing or exchange of electrons between adsorbent and adsorbate, was able to well describe the adsorption kinetics [21]. Therefore, the model was applied in this work with its expression as

$$\frac{t}{q_t} = \frac{1}{v_0} + \frac{t}{q_e} \quad (1)$$

where q_e and q_t (mg g^{-1}) is the amount of adsorbed heavy metal at equilibrium and at time t, respectively, v_0 (mg g^{-1} min^{-1}) is the initial sorption rate; $v_0 = k_2 q_e^2$, in which k_2 (g mg^{-1} min^{-1}) is the rate constant.

Plotting t/q_t against t gives a straight line to reflect the goodness-of-fit (Fig. 8). It indicated that the experimental data could be described by the pseudo-second-order model with correlation coefficients $r^2 > 0.99$ for all concentrations. The corresponding rate constant k_2 was 0.1140, 0.0425, 0.0127, and 0.0110 g mg^{-1} min^{-1}, respectively, for 100, 200, 400 and 500 mg L^{-1} Cr(VI) adsorption. The rate constant decreased with the increase of initial Cr(VI) concentration, which was consistent with the previous research [22].

3.4. Adsorption isotherms and thermodynamic evaluation

The adsorption isotherms at 35 °C, 25 °C, and 15 °C were evaluated respectively, by changing the initial concentration of Cr(VI) from 50 to 500 mg L^{-1}. The calculated parameters based on Langmuir adsorption model were listed in Table 1. The Langmuir adsorption model, which assumes that all the binding sites are equal and the adsorbent surface is homogeneous, is expressed as

$$q_e = \frac{q_m K_L C_e}{(1 + K_L C_e)} \quad (2)$$

where q_e (mg g^{-1}) is the amount of Cr(VI) adsorbed at equilibrium; q_m (mg g^{-1}) is the maximum adsorption capacity; C_e (mg L^{-1}) is the equilibrium solute concentration, and K_L is the equilibrium constant (L mg^{-1}) related to adsorption energy.

Besides Langmuir model, Freundlich sorption model was also applied to analyze the experimental data. It is commonly presented as

$$q_e = K_F C_e^{1/n} \quad (3)$$

where K_F and n are the Freundlich constants related to adsorption capacity and adsorption intensity, respectively [21].

Table 1
Langmuir and Freundlich model parameters for Cr(VI) adsorption at different temperatures.

	Langmuir model				Freundlich model		
	q_m (mg g^{-1})	K_L (L mg^{-1})	K_L (L mol^{-1})	r^2	K_F	n	r^2
35 °C	74.07	0.0684	3.56	0.991	11.74	3.27	0.925
25 °C	78.13	0.111	5.77	0.989	18.13	3.46	0.969
15 °C	83.33	0.125	6.50	0.988	20.85	3.75	0.934

Table 2
Values of thermodynamic parameters for Cr(VI) removal using PEI-MNPs.

Temperature (K)	$\ln K_L$	ΔG (kJ mol^{-1})	ΔH (kJ mol^{-1})	ΔS (J mol^{-1} K^{-1})
308	1.2697	−3.251	−22.04	−60.46
298	1.7526	−4.342		
288	1.8718	−4.481		

The Langmuir model provided the best results for these sorts of lines based on the correlation coefficients ($r^2 > 0.98$). The maximum adsorption capacities (q_m) for Cr(VI) by PEI-MNPs at 35–15 °C were 74.07–83.33 mg g^{-1}, which was much higher than that of unmodified MNPs (q_m = 12.66 mg g^{-1} at 25 °C). The high capacity indicated its potential application in Cr(VI) removal from wastewater. The correlation coefficients of the Freundlich model under all temperatures were more than 0.92. The best-fit Freundlich parameter n was in the range of 2–10, suggesting a favourable adsorption process [23].

The adsorption isotherms were carried out under different temperatures, thus thermodynamic evaluation was able to be done based on it. The thermodynamic parameters of the adsorption process such as change in standard free energy (ΔG), enthalpy (ΔH), and entropy (ΔS) can be obtained using the following equations [24]

$$\Delta G = -RT \ln K_L \quad (4)$$

$$\ln K_L = \frac{\Delta S}{R} - \frac{\Delta H}{RT} \quad (5)$$

where K_L is the Langmuir constant (L mol^{-1}), R is the ideal gas constant (8.31 J mol^{-1} K^{-1}), and T is the absolute temperature. ΔH and ΔS could be obtained from the slope and intercept of van't Hoff plots of $\ln K_L$ versus $1/T$. The values of the thermodynamic parameters are presented in Table 2.

The negative values of the ΔG and ΔH meant that the adsorption was a spontaneous exothermic process; and consequently a lower temperature was favourable to the reaction, which might explain the increase of q_m with the decrease of temperature. The negative ΔH was noteworthy, since Li et al. [22] and Bayramoglu [25] had reported the positive ΔH in investigation of Cr(VI) adsorption. The phenomenon might be attributed to the electrostatic interaction between Cr(VI) and the PEI-MNPs, which is an exothermic process, resulting in the observation of negative ΔH. The negative entropy changes (ΔS = −60.46 J mol^{-1} K^{-1}) indicated that the order degree increased during the adsorption process.

3.5. Effect of common ions

Various ions exist in wastewater. The presence of other solutes may reduce the adsorption of any given adsorbate to some extent. In addition, the uptake of the other ions influences the recovery of Cr(VI) directly. Thus, K^+, Na^+, Ca^{2+}, and Cu^{2+}, as well as the anions of Cl^- and NO_3^-, which are the commonly coexisting ions with Cr(VI), were chosen for study. Fig. 9 revealed that the effect of the studied common ions on the adsorption of Cr(VI) was considerably insignificant, even if the ions concentration increased to double, implying that they did not compete for the active sites with Cr(VI) [26]. It is noteworthy that some PEI modified adsorbents adsorbed Cu^{2+} effectively [4,12], much different with this work. The distinct performances were mainly due to the different adsorption mechanisms, which was electrostatic interaction and chelating adsorption respectively, under different solution pH. Therefore, selective adsorption of Cr(VI) can be achieved by the prepared adsorbent.

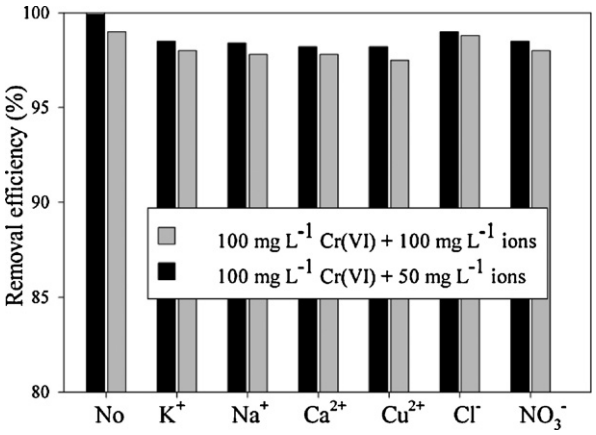

Fig. 9. Effect of coexisting ions on the removal of Cr(VI) by PEI-MNPs (adsorbent dose 0.08 g, pH value 2.2, contact time 30 min, temperature 25 °C).

Furthermore, actual wastewater (from an electronics factory) with Cr(VI) concentration of 37.98 mg L^{-1} was reduced to 0.375 mg L^{-1} after adding 2.67 g L^{-1} adsorbent for 30 min treating, indicating the feasibility of removing Cr(VI) from multi-component effluent using the PEI-MNPs.

3.6. Stability and regeneration

The PEI-MNPs were exposed to different concentrations of HCl or NaOH for 3 h. The leached Fe content and the adsorption capacity of the treated adsorbent were determined, respectively. No significant Fe leaching was observed in acid or alkali solution with concentration range of 0.2–1 mol L^{-1} (Table 3). The magnetization of these adsorbents was strong enough for magnetic separation. In contrast, the naked Fe_3O_4 was dissolved completely in 1 mol L^{-1} HCl. Furthermore, the adsorbent could be preserved for five months at room temperature without deterioration. The excellent stability could be due to the formed γ-Fe_2O_3 on the surface of nanoparticles, which has similar magnetic properties to Fe_3O_4 but better chemical stability to protect inner Fe_3O_4 [15,16].

A slight increase in removal efficiency for acid incubated adsorbent (Table 3) was probably due to the surface protonation of the adsorbent caused by HCl treatment. Since the suppressed Cr(VI) adsorption was found at high pH (confirmed in Section 3.2), alkali wash was a feasible approach to regenerate the Cr(VI) loaded adsorbent. Therefore, 0.02 mol L^{-1} NaOH solution was adopted for regeneration, and the regenerated adsorbent was used for six consecutive cycles. The removal efficiency of Cr(VI) did not change significantly during the repeated adsorption–desorption operations (decreased only 9% in the sixth cycle), suggesting that the regeneration method was quite effective.

Table 3
Leached Fe rate and Cr(VI) removal efficiency of adsorbent after treated by different concentrations HCl and NaOH solution.

	HCl (mol L^{-1})				NaOH (mol L^{-1})			Untreated
Concentration	0.2	0.5	1	2	4 0.2	0.5	1	
Leaching rate (%)	2.74	4.68	21.6	58.9	100 0.15	0.23	0.18	0
Removal rate (%)	88.4	91.0	92.1	88.6	87.0	85.4	88.6	86.8

4. Conclusions

In this work, MNPs with enhanced stability were prepared by calcining Fe_3O_4 to form a protecting shell of γ-Fe_2O_3. PEI was grafted to the nanoparticle to develop a positive surface charged adsorbent for effective removal of anionic Cr(VI) mainly by electrostatic interaction. The removal efficiency was highly pH dependent and the optimal adsorption occurred at pH of 2–3. Adsorption of Cr(VI) was very fast, only 30 min was needed to reach equilibrium. The saturated capacity of 74.07–83.33 mg g^{-1} was obtained in the temperature range of 35–15 °C. Thermodynamic evaluation revealed that the adsorption process was spontaneous and exothermic. The competitive studies showed the effect of common coexisting ions was negligible on Cr(VI) adsorption. The regeneration studies revealed that the adsorbent can be used for six consecutive adsorption–desorption cycles without significant loss of adsorption capacity.

Acknowledgments

This study was financially supported by the Program for Changjiang Scholars and Innovative Research Team in University (IRT0719), the National Natural Science Foundation of China (50978088, 51039001, 50608029), the Hunan Key Scientific Research Project (2009FJ1010), the Hunan Provincial Natural Science Foundation of China (10JJ7005), the Hunan Provincial Innovation Foundation For Postgraduate (CX2009B080, CX2010B157) and the Fundamental Research Funds for the Central Universities, Hunan University.

References

[1] E. Finocchio, A. Lodi, C. Solisio, A. Converti, Chromium (VI) removal by methylated biomass of *Spirulina platensis*: the effect of methylation process, Chem. Eng. J. 156 (2010) 264–269.
[2] S.B. Deng, Y.P. Ting, Polyethylenimine-modified fungal biomass as a high capacity biosorbent for Cr(VI) anions: sorption capacity and uptake mechanisms, Environ. Sci. Technol. 39 (2005) 8490–8496.
[3] G.Q. Chen, W.J. Zhang, G.M. Zeng, J.H. Huang, L. Wang, G.L. Shen, Surface-modified *Phanerochaete chrysosporium* as a biosorbent for Cr(VI) contaminated wastewater, J. Hazard. Mater. 186 (2011) 2138–2143.
[4] Y. Chen, B. Pan, H. Li, W. Zhang, L. Lv, J. Wu, Selective removal of Cu(II) ions by using cation-exchange resin-supported polyethyleneimine (PEI) nanoclusters, Environ. Sci. Technol. 44 (2010) 3508–3513.
[5] S.E. Bailey, T.J. Olin, R.M. Brika, D.D. Adrian, A review of potentially low-cost sorbents for heavy metals, Water Res. 33 (1999) 2469–2479.
[6] J.F. Liu, Z.S. Zhao, G.B. Jiang, Coating Fe_3O_4 magnetic nanoparticles with humic acid for high efficient removal of heavy metals in water, Environ. Sci. Technol. 42 (2008) 6949–6954.
[7] Y.C. Chang, D.H. Chen, Preparation and adsorption properties of monodisperse chitosan-bound Fe_3O_4 magnetic nanoparticles for removal of Cu(II) ions, J. Colloid Interface Sci. 283 (2005) 446–451.
[8] W. Yantasee, C.L. Warner, T. Sangvanich, R.S. Addleman, T.G. Carter, R.J. Wiacek, G.E. Fryxell, C. Timchalk, M.G. Warner, Removal of heavy metals from aqueous systems with thiol functionalized superparamagnetic nanoparticles, Environ. Sci. Technol. 41 (2007) 5114–5119.
[9] Y. Zhang, G.M. Zeng, L. Tang, D.L. Huang, X.Y. Jiang, Y.N. Chen, A hydroquinone biosensor using modified core-shell magnetic nanoparticles supported on carbon paste electrode, Biosens. Bioelectron. 22 (2007) 2121–2126.
[10] A.H. Lu, W.C. Li, N. Matoussevitch, B. Spliethoff, H. Bonnemann, F. Schuth, Highly stable carbon-protected cobalt nanoparticles and graphite shells, Chem. Commun. 1 (2005) 98–100.
[11] Q. Gao, F.H. Chen, J.L. Zhang, G.Y. Hong, J.Z. Ni, X. Wei, D.J. Wang, The study of novel Fe_3O_4@γ-Fe_2O_3 core/shell nanomaterials with improved properties, J. Magn. Magn. Mater. 321 (2009) 1052–1057.
[12] Y. Pang, G.M. Zeng, L. Tang, Y. Zhang, Y.Y. Liu, X.X. Lei, Z. Li, J.C. Zhang, PEI-grafted magnetic porous powder for highly effective adsorption of heavy metal ions, Desalination (2011), doi:10.1016/j.desal.2011.08.001.
[13] H.T. Hai, H. Kura, M. Takahashi, T. Ogawa, Facile synthesis of Fe_3O_4 nanoparticles by reduction phase transformation from γ-Fe_2O_3 nanoparticles in organic solvent, J. Colloid Interface Sci. 341 (2010) 194–199.
[14] J. Li, X.Y. Qiu, Y.Q. Lin, X.D. Liu, R.L. Gao, A.R. Wang, A study of modified Fe_3O_4 nanoparticles for the synthesis of ionic ferrofluids, Appl. Surf. Sci. 256 (2010) 6977–6981.
[15] J.Y. Zhan, G.F. Tian, L.Z. Jiang, Z.P. Wu, D.Z. Wu, X.P. Yang, R.G. Jin, Superparamagnetic polyimide/γ-Fe_2O_3 nanocomposite films: preparation and characterization, Thin Solid Films 516 (2008) 6315–6320.
[16] J.J. Bergmeister, L.T. Taylor, Synthetic strategies in the formation of iron-modified polyimide films, Chem. Mater. 129 (1992) 729–734.
[17] B.M. Weckhuysen, I.E. Wachs, R.A. Schoonheydt, Surface chemistry and spectroscopy of chromium in inorganic oxides, Chem. Rev. 96 (1996) 3327–3349.
[18] G. Bayramoglu, G. Celik, M. Yılmaz, M.Y. Arica, Modification of surface properties of Lentinus sajor-caju mycelia by physical and chemical methods: evaluation of their Cr^{6+} removal efficiencies from aqueous medium, J. Hazard. Mater. 119 (2005) 219–229.
[19] C.H. Weng, J.H. Wang, C.P. Huang, Adsorption of Cr(VI) onto TiO_2 from dilute aqueous solutions, Water Sci. Technol. 35 (1997) 55–62.
[20] S.B. Lalvani, A. Hubener, T.S. Wiltowski, Chromium adsorption by lignin, Energy Sources 22 (2000) 45–56.
[21] L.Y. Wang, L.Q. Yang, Y.F. Li, Y. Zhang, X.J. Ma, Z.F. Ye, Study on adsorption mechanism of Pb(II) and Cu(II) in aqueous solution using PS-EDTA resin, Chem. Eng. J. 163 (2010) 364–372.
[22] Y.J. Li, B.Y. Gao, T. Wu, D.J. Sun, X. Lia, B. Wang., F.J. Lu, Hexavalent chromium removal from aqueous solution by adsorption on aluminum magnesium mixed hydroxide, Water Res. 43 (2009) 3067–3075.
[23] A. Shahbazi, H. Younesia, A. Badiei, Functionalized SBA-15 mesoporous silica by melamine-based dendrimer amines for adsorptive characteristics of Pb(II), Cu(II) and Cd(II) heavy metal ions in batch and fixed bed column, Chem. Eng. J. 168 (2011) 505–518.
[24] T. Fan, Y.G. Liu, B.Y. Feng, G.M. Zeng, C.P. Yang, M. Zhou, H.Z. Zhou, Z.F. Tan, X. Wang, Biosorption of cadmium(II), zinc(II) and lead(II) by *Penicillium simplicissimum*: isotherms, kinetics and thermodynamics, J. Hazard. Mater. 160 (2008) 655–661.
[25] G. Bayramoglu, M.Y. Arica, Adsorption of Cr(VI) onto PEI immobilized acrylate-based magnetic beads: Isotherms, kinetics and thermodynamics study, Chem. Eng. J. 139 (2008) 20–28.
[26] J. Hu, M.C. Lo, G.H. Chen, Adsorption of Cr(VI) by magnetite nanoparticles, Water Sci. Technol. 50 (2004) 139–146.